Physica Scripta

An International Journal for Experimental and Theoretical Physics

Dear Author,

Please find attached a PDF of your article that has appeared in issue 70 pt 4 of Physica Scripta. This file has been optimised for viewing on screen, but can be printed off. If you would like a version of this file, optimised for printing, or would like to purchase a number of printed copies of your paper, please contact me.

Best Wishes,

Audry Samuels
Journal Controller
Marston Digital
Omega Park
Collet
Didcot
OX11 7AW
email: samuelsa@lrl.com
voice: +44 1235 518700
fax: +44 1235 515777
web: http://www.physica.org

Editorial office	Telephone	Telefax	Electronic Mail	Home Page
Physica Scripta **The Royal Swedish Academy of Sciences** **Box 50005** **S-104 05 Stockholm, Sweden**	+46-(0)8-673 95 00	+46-(0)8-673 95 90	physica@kva.se	http://www.physica.org

Physica Scripta. Vol. 70, 251–256, 2004

Classical Structures Arising in the Autoionization of He

S. Otranto* and G. Gasaneo

Departamento de Física, Universidad Nacional del Sur and Consejo Nacional de Investigaciones Científicas y Técnicas, 8000 Bahía Blanca, Buenos Aires, Argentina

Received November 17, 2003; revised version received March 1, 2003; accepted March 12, 2004

PACS Ref: 34.50Fa

Abstract

In this work, a classical mechanics study of the autoionization process induced by ion impact is performed. The electron distribution in momentum space is obtained and compared with the results of the continuum distorted wave quantum theory. Typical structures arising in quantum and classical treatments are identified and compared. Oscillatory profiles for the autoionization spectrum are obtained within the present classical picture, in contrast with existing models which attach them to a purely quantum behavior.

1. Introduction

One of the processes observed during the collision of charged particles and photons with atoms is the ionization of a single electron, leaving the remaining target with one extra unit of plus charge. Two main mechanisms can take place within this process: direct ionization and two step *Auger effect*. During the collision the incident particle (or photon) can leave the target atom in an excited state which decays in a radiation-less form by the emission of an electron to the continuum. When a two electron atom is involved the process is known as autoionization. Usually, the denomination *Auger effect* is used for electron emission induced by a primary inner-shell ionization of many-electron atoms, in honour to P. Auger who discovered it in 1925 [1]. In this case, the electron emission is a consequence of the rearrangement of the atom which after the inner-shell ionization becomes unstable. In this paper we will concentrate in the autoionization process and for practical purposes we will refer to the He atom.

A difference between the electrons emitted by auto-ionization and other processes is that the energy is quite well defined in the former. This is mainly due to the spontaneous emission from a doubly excited state embedded in the continuous spectra of the ground state of a one electron atom. Thus, the energy can only present a small dispersion corresponding to the line width $\hbar/\Gamma$. If the autoionization is induced by photon impact, the angular distribution of the electron depends only on the symmetry of the autoionizing state.

The autoionization induced by ion impact presents a series of substantial differences with that induced by photons. The electrons are emitted not only in presence of the residual target but of the projectile. Thus, changes should be expected in the energy and angular distribution due to the presence of the projectile instead of the isotropic behavior typical of the process reached by photon impact. The first observed effect is a shift on the emission energy due to the inclusion of the potential energy of the electron in the field of the projectile. Besides, an asymmetric profile appears in the typical isotropic Lorenzian. These effects were discussed by Barker and Berry in 1966 in a classical model built upon phenomenological considerations [2]. For more than a decade, this turned the only available model to describe the autoionization induced by ion impact. In 1977, Devdariani *et al*. developed the first quantum mechanical model for this process [3]. In their pioneering work, they made the same consideration that Barker and Berry performed in the classical context. They assumed the projectile to affect the electron energy but not its trajectory. The eikonal model of van der Straten and Morgenstern in 1986 represents the first attempts to introduce the post collisional interaction (PCI) between the emitted electron and the projectile [4]. Finally in 1989, the continuum distorted wave (CDW) of Barrachina and Macek [5] successfully predicted the existence of a Coulomb focusing mechanism which was experimentally corroborated in the same year by Swenson *et al*. [6]. This model with its subsequent improvements [7–9] took account of the Stark effect (which is important when the impinging ion energy is rather low) and the distorting effects the projectile induces on the excited state modifying its lifetime.

Meanwhile, the classical description of the process was not laid aside. In 1989 and 1991 Swenson *et al*. employed a Coulomb path interference mechanism in order to give a classical description of the Coulomb focusing [6,10]. They concluded that this effect is a consequence of electrons emitted in the forward direction at slightly different emission times that could emerge from the collision, after following different paths, with the same asymptotic velocity. Furthermore, this Coulomb path interference thus represents an ion-atom collision analog to classic double-slit electron scattering.

Recently, another semi-classical analysis showed that the interference structures of CDW spectral lines could be interpreted in terms of *nearside–farside* scattering, which was first used to describe elastic reactions of spin-zero nuclei [11]. Decomposition is possible of the autoionization amplitude in two terms which can be related to trajectories which have traveled along one or the other side of the interaction potential suffering a positive or negative deflection. On the other hand, Kunikeev and Senashenko [12] interpreted oscillatory structures in the autoionization peaks as an interference between waves that are and are not scattered by the projectile. As a result, many possible interpretations have been employed to describe this feature from both classical and quantum point of view. The purpose of the present article is to clarify this point.

In this work, we concentrate on giving a classical picture of the emitted electron trajectory. We take a different point of view and perform a simulation of the autoionization

* e-mail: sotranto@uns.edu.ar

process in classical terms. In the next section, we show how the electron distribution in momentum space is obtained. For this purpose, we use many well known concepts in classical mechanics to solve the two-body Coulomb problem with particular initial conditions. The dynamical evolution of electrons emitted from a moving point-*like* source is studied. The trajectories as well as the final velocities of the electrons are given. In Section 3, the autoionization process is considered. The electron distributions in momentum space are obtained and compared with those resulting from the CDW quantum theory. The purely classical structures are identified. Oscillations in the autoionization profile due to the simple superposition of classical structures are obtained and discussed. Main results are summarized. Finally some conclusions are drawn. Atomic units are used throughout this work unless explicitly stated.

2. The electron distribution in momentum space for the coulomb problem

Let us consider the autoionization of an atom induced by ion impact. We assume that the projectile leaves the atom in a doubly-excited state. Within the PCI-scheme, the atom spontaneously decays in the presence of the projectile. So, once the electron has been emitted by the atom, it evolves under the projectile field. The dynamics of the electron can be better analyzed in a projectile reference system. In the PCI-scheme the time dependent problem of an electron in two moving centers reduces to a time-independent problem of one electron in the field of only one center (the projectile). The time dependence leads to a time-dependent initial condition for each of the electrons emitted by the autoionizing atom.

We study the trajectory of an emitted electron which only interacts with the projectile field (post collisional interaction scheme). This implies a considerable simplification but allows for an exact treatment of the problem. The initial conditions of the problem are given by defining the initial distance r_0 of the emitted electrons to the projectile and the emission velocity v_0 and angle θ_0, measured with respect to the incidence direction z. The velocity of the projectile is $\boldsymbol{v}_P$. Placing the reference system in the projectile, the energetic balance reads

$$\tfrac{1}{2}mv^2 = \tfrac{1}{2}m\boldsymbol{v}_{\text{emis}}^2 - \frac{Z_P}{r_0} = E_0. \tag{1}$$

$\boldsymbol{v}_{emis}$ represents the relative velocity of the emitted electron to the moving projectile and it is defined by $\boldsymbol{v}_{\text{emis}} = \boldsymbol{v}_0 - \boldsymbol{v}_P$. From Eq. (1) the asymptotic velocity v could be obtained, being clearly a function of the initial distance and the projectile velocity.

The orbit equation for the Coulomb problem is well known in classical dynamics and is given by [13]

$$\frac{p}{r} = \pm 1 + e\cos\phi \tag{2}$$

where the upper (lower) sign corresponds to the interaction with an attractive (repulsive) projectile. Here p and e are usually referred to as the parameter and eccentricity of the orbit,

$$p = \frac{l_0^2}{mZ_P}, \tag{3}$$

$$e = \left[1 + \frac{2E_0 l_0^2}{mZ_P^2}\right]^{1/2}. \tag{4}$$

They are given in terms of the modulus l_0 of the angular momentum, which referred to the emission instant is given by $\boldsymbol{l}_0 = m\boldsymbol{r}_0 \times \boldsymbol{v}_{\text{emis}}$ and the projectile charge Z_p.

The perihelion is defined as the point of the orbit that is closest to the center, the distance being

$$r_{\min} = \frac{p}{e \pm 1} \tag{5}$$

with the upper (lower) sign again corresponding to the interaction with an attractive (repulsive) projectile.

The angle ϕ gives the asymptotic angle of the orbit measured from the perihelion and is given by:

$$\phi = \cos^{-1}\left(\mp\frac{1}{e}\right). \tag{6}$$

Let us consider the electron orbits for a projectile fixed at a certain distance R from the emitter, v_{emis} fixed and different emission angles. The situation in which $mv_{\text{emis}}^2/2 < Z_p/r_0$ leads for the different emission angles to closed elliptic orbits, all crossing in the point where the electron "source" is located. For $mv_{\text{emis}}^2/2 > Z_p/r_0$ the different emission angles lead to hyperbolic orbits, all of them joining in the same point r_0 (see Fig. 1). The Runge–Lenz vector is defined by [14]

$$\boldsymbol{A} = m\boldsymbol{v} \times \boldsymbol{l} - mZ_p\hat{\boldsymbol{r}}, \tag{7}$$

and its initial definition $\boldsymbol{A}_0 = m\boldsymbol{v}_{\text{emis}} \times \boldsymbol{l}_0 - mZ_p\hat{\boldsymbol{r}}_0$ gives the perihelion position for each emission angle. For large

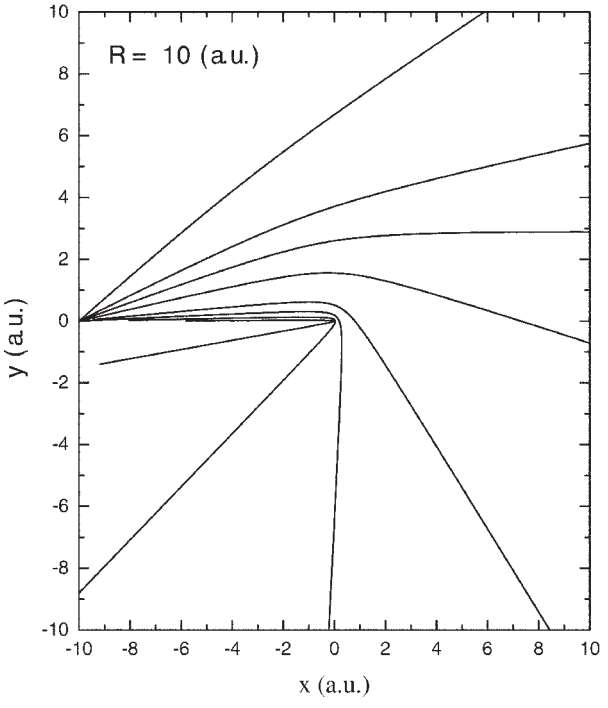

Fig. 1. Electron trajectories in the field of a fixed center at 10 a.u. of the emitter for different emission angles in the projectile frame.

angles, the trajectories of the emitted electrons are slightly modified, but they bend strongly towards the projectile for decreasing emission angles. It is possible to identify a limit angle θ_G for which the trajectories of the emitted electrons are parallel to the source-projectile line. All the trajectories coming from emission angles smaller than θ_G overtake the projectile and cross ahead of its trajectory. So, we can distinguish those trajectories with $\theta_0 > \theta_G$ overcoming the projectile trajectory from those with $\theta_0 < \theta_G$ which do not overcome it. Of course there exists a θ_G for each distance R which is given by

$$\theta_G = \arccos\sqrt{1 - \frac{Z_P/R}{1/2m\boldsymbol{v}_{\text{emis}}^2}}. \tag{8}$$

This angle, as we shall see, is the angle corresponding to the *glory effect*. Through Eq. (8) we can note that θ_G decreases for increasing values of R, and in the limit of $R \longrightarrow \infty$ it becomes zero.

The scattering cross section usually defined in terms of impact parameters and assuming that the impinging particles form a beam coming from infinity. In the problem of our concern, the emitter could be located at an arbitrary distance from the Coulomb center and the emission occurs in all directions. These differences in the definition of the problem lead to a modified differential cross section:

$$\sigma(\Theta) = \frac{\sin\theta_0}{\sin\Theta}\left|\frac{\mathrm{d}\theta_0}{\mathrm{d}\Theta}\right| \tag{9}$$

where Θ is the scattering angle and the sum runs over all the emission angles θ_0 which lead to the same asymptotic angle Θ. When compared with the usual definition [13,14], $\sin\theta_0$ replaces the impact parameter and the derivative of θ_0 with respect to Θ replaces the impact parameter derivative with respect to Θ. Although this is an adimensional quantity, it could be considered a differential cross section since it represents the number of scattered electrons in a given solid angle per unit time and incident flux. The study of the divergences of this cross section could be associated with two well-known optical effects: the *glory effect* given by $\sin\Theta = 0, \theta_0 \neq 0, \mathrm{d}\theta_0/\mathrm{d}\Theta \neq 0$ and the *rainbow effect* which corresponds to $\mathrm{d}\theta_0/\mathrm{d}\Theta \to \infty, \theta_0 \neq 0$. In the case considered here, the glory (rainbow) effect is reached by positive (negative)-ion impact and both of them leave, as we shall see in the next section, a noticeable fingerprint on the autoionization electronic distributions. However, in the present analysis we dispense of the use of this scattering cross section and we concentrate on the asymptotic part of the orbits instead.

In order to obtain the asymptotic velocity vector we must define its direction. In the following, we measure the asymptotic angle Θ from the z axis (the beam direction) counterclockwise. In order to determine this angle, we must take account of the angle α between the perihelion and the emitter. The Laplace–Runge–Lenz vector defined in terms of the initial conditions allows us to define the angle α as follows

$$\alpha = \cos^{-1}\left(\frac{\boldsymbol{A}_0 \cdot \boldsymbol{r}_0}{A_0 r_0}\right). \tag{10}$$

In this sense, Θ results are defined by the initial conditions through the angles α and ϕ.

We assume the orbit to take place in the z, x plane. Then, the asymptotic angle Θ could be expressed by sections, according to the respective values taken by the components z, x of the emission velocity vector $\boldsymbol{v}_{\text{emis}}$:

$$(\boldsymbol{v}_{\text{emis}})_z > 0, \quad (\boldsymbol{v}_{\text{emis}})_x > 0, \quad \Theta = \pi - (\phi + \alpha),$$

$$(\boldsymbol{v}_{\text{emis}})_z > 0, \quad (\boldsymbol{v}_{\text{emis}})_x < 0, \quad \alpha + \phi < \pi, \quad \Theta = \pi + (\phi + \alpha),$$

$$(\boldsymbol{v}_{\text{emis}})_z > 0, \quad (\boldsymbol{v}_{\text{emis}})_x < 0, \quad \alpha + \phi > \pi, \quad \Theta = (\phi + \alpha) - \pi,$$

$$(\boldsymbol{v}_{\text{emis}})_z < 0, \quad (\boldsymbol{v}_{\text{emis}})_x > 0, \quad \Theta = \pi - (\phi - \alpha),$$

$$(\boldsymbol{v}_{\text{emis}})_z < 0, \quad (\boldsymbol{v}_{\text{emis}})_x < 0, \quad \Theta = \pi + (\phi - \alpha).$$

From these expressions and the orbits shown in Fig. 1, we can conclude that for $(\boldsymbol{v}_{\text{emis}})_z < 0$ the orbit does not contain a perihelion since it has already been passed. Thus, we have obtained the asymptotic velocity vector of an electron emitted under the above mentioned initial conditions seen from the projectile frame. In order to express this vector in the emitter frame, we must simply add the projectile velocity vector.

3. The autoionization problem

In this section we describe the main features corresponding to our classical simulation of the autoionization process. We will consider the trajectory of each emitted electron and evaluate its asymptotic velocity. By taking a large enough number of trajectories we compose the electron spectra corresponding to the autoionization process.

In the previous section, we have not made any assumption about the way in which it was emitted. We have just assumed emission in all directions and at a time-dependent distance. According to the quantum theory [15], if the autoionization process takes place due to excitation of the ground state to an autoionizing state by photon absorption, the electron intensity profile I of the spectra is given by the Lorenzian,

$$I = \frac{\Gamma^2}{\Gamma^2 + 1/4\left(v_e^2 - \widetilde{v}_0^2\right)^2} \tag{11}$$

where Γ is the full width at half maximum of the Lorenzian. Then, we will use this velocity profile to calculate the initial electron velocity $\boldsymbol{v}_0$ according to a Lorenzian distribution,

$$\boldsymbol{v}_0 = \left[\widetilde{v}_0 \pm 2\Gamma\left(\frac{1}{x} - 1\right)^{1/2}\right] \tag{12}$$

with x a real number between 0 and 1. The velocity $\widetilde{v}_0$ is the velocity acquired by the emitted electron as the second one decays forming He^+. For the He atom, and for the autoionizing states $2s^2(^1S), 2p^2(^1D)$, and $2s2p(^1P)$ the values for Γ are 0.00507, 0.00265 and 0.0014 a.u. and their corresponding electron velocities $\widetilde{v}_0$ are 1.5646, 1.6106 and 1.6168 a.u. [7].

According to Barker and Berry, the probability that the electron has been emitted at the time t after the excitation has occurred is given by

$$P_{BB}(t) = 1 - e^{-\Gamma t}. \quad (13)$$

We use this law to weight the electron emission at different distances of the projectile. Letting y be a random variable uniformly distributed between 0 and 1, and since $t = r_0/v_P$ we obtain the following distribution for the initial position of the projectile,

$$r_0 = \frac{v_P}{\Gamma} |\log(1 - y)|. \quad (14)$$

Using the velocity and distance distributions, we build the electron distribution in the velocity space of the electron considered in the emitter frame, as shown in Fig. 2. A total of 25000 electrons have been emitted from the $2s^2(^1S)$ autoionizing state sorting their velocities and projectile distances according to the distributions mentioned above. Three different velocities have been considered (0.6, 1.2 and 1.8 a.u.) for an attractive projectile of charge $Z_P = 1$. For comparison, a contour plot (in logarithmic scale) for the CDW results of the quantum theory have been included [9]. Two structures observed in the quantum calculations appear also in the classical one: the autoionization and the binary rings. We should note that the binary ring has not been mentioned previously in the literature with exception to the work of Caputti [16]. In this work, the quantum transition amplitude was separated in two parts following the procedure proposed by Kunikeev and Senashenko [12] and

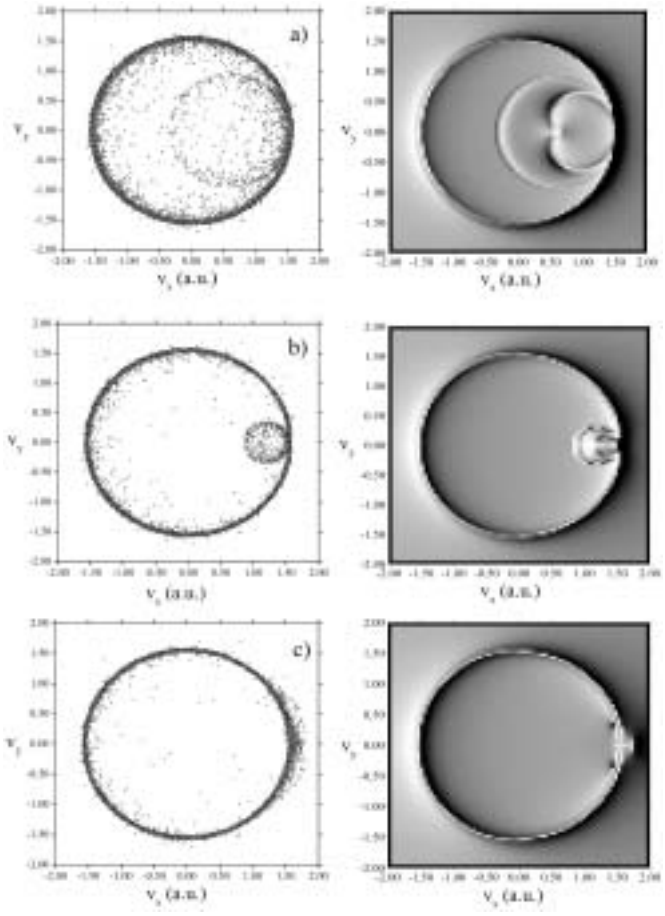

Fig. 2. Electron distribution in velocity space considered in the emitter frame for a positively charged projectile. Left: present model; right: CDW model. Three projectile velocities are considered: 0.6, 1.2 and 1.8 a.u.

one of the structures was recognized as the binary ring. The autoionization ring represents electrons that seeing the projectile field deflect their trajectories, but none of them bends it enough to overcome the projectile trajectory. In the cases considered in Fig. 2(a) and (b), the electron velocity is greater than the projectile's. As we mentioned in the previous section, for each projectile distance there exists a glory angle α_G. All the trajectories with emission angles smaller than this glory angle will cross the projectile trajectory. In the plots of Fig. 2(a) and (b), the structure observed inside the autoionization ring results from the accumulation of all these electrons. Overcoming the projectile trajectory ($\Theta = 0$) means a strong interaction between the electron and the projectile. The energy change from scattering off a heavy particle must be negligible. As a consequence the electrons diminish their velocity forming the binary ring. The electrons emitted with small emission angles transfer more energy to the projectile than those emitted with an angle close to the glory. In Fig. 2(c), the projectile velocity is greater than that of the autoionization electrons, so now the binary ring is not allowed and the electrons are pulled in the forward direction out of the autoionization ring. This is also evident in the CDW theory where a minimum of intensity is observed on the autoionization ring [17]. Besides the classical effects mentioned, the CDW theory adds other non-classical structures. One of them is the continuum capture to the continuum (ECC) peak, situated on the projectile velocity [18,19]. This divergence of intensity in the distribution, represents a zero energy resonance for the electrons which travel with zero relative velocity respect the projectile. Another non-classical structure is that "crab"-like form, which connects the ECC peak with the focusing peak in the forward direction. A discussion about the origin of these structures will be given in another paper. A particular situation is when the emission angle is close to or coincides with the glory angle. As we mentioned in the previous section, in this situation the cross section of Eq. (9) diverges. Thus, for each emission angle a divergence will be observed. The minimal distance from which it occurs is given by $(Z_P/R)/(1/2)mv^2_{\text{emis}} = 1$, and this defines a maximum angle. The minimal angle is $\theta_G = 0$ and corresponds to the situation where the electron emission happens when the projectile is at an infinite distance from the target. So, a large amount of electrons will accumulate in the forward direction as a consequence of the divergence occurring for each distance. This gives rise to a structure known as focusing peak and it appears on the binary ring and close to the forward direction. According to the weighted velocity and emission time given by Eqs. (12) and (14), the electrons emitted at different times (or equivalently different distances of the projectile) contribute differently in the electron spectra. The electron emission at small projectile distances is less probable than that occurring at intermediate and large ones. So there are less electrons contributing to the glory effect for large angles and this produces an angular profile. Since we are considering a finite number of electrons, the glory does not lead to a divergence but a maximum. In Fig. 3 a we plot the angular profile of the binary where the focusing is clearly visible.

In Figs. 3(b) and 4 the repulsive projectile case is considered. In Fig. 3(b) we show the angular profile of the

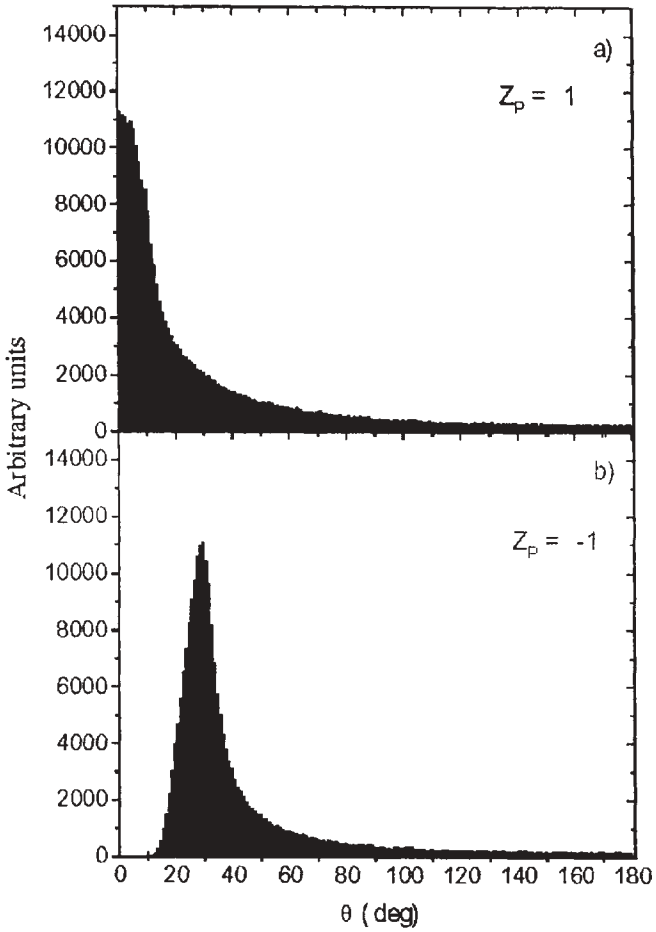

Fig. 3. Angular profile of the binary ring in the projectile frame. (a) and (b) positively and negatively charged projectile respectively.

binary ring seen from the projectile frame for negatively charged projectiles. A total absence of electrons in the forward direction is obtained. This behavior has been explained in terms of optics-analog effects as the rainbow effect [20]. The three projectile velocities considered in Fig. 4 are as mentioned above. It could be observed that electrons are pulled outside of the binary and autoionization rings. The quantum theory again exhibits the non-classical structure when the electron velocity is equal to the projectile one, leading in this case to zero intensity in the distribution. The total absence of electrons emitted in the projectile direction is also clearly noticeable. The histogram made for $v_P = 1.2$ a.u, $Z_P = 1$ shown in Fig. 5, represents the intensity profile for the asymptotic angles 0, 5 and 10 degrees. The contribution of the binary ring could be clearly appreciated as also the asymmetry of the autoionization peak, first observed by Barker and Berry, due to the projectile distorting effect. Recently, an analysis based on the CDW model explained that certain oscillations in the profiles could be due to the interference between waves that have and have not been scattered by the receding projectile [12]. The presence of an apparently oscillating profile within the classical description, shows to be a consequence of the simple accumulation of separate structures, i.e. the binary and the autoionization rings. Our classical results then show that similar *oscillatory-like*

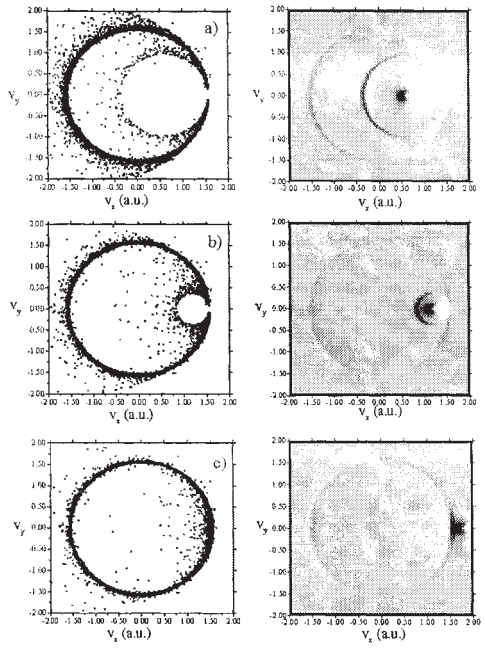

Fig. 4. Electron distribution in velocity space considered in the emitter frame for a negatively charged projectile. Left: present model; right: CDW model. The projectile velocities are as in Fig. 2.

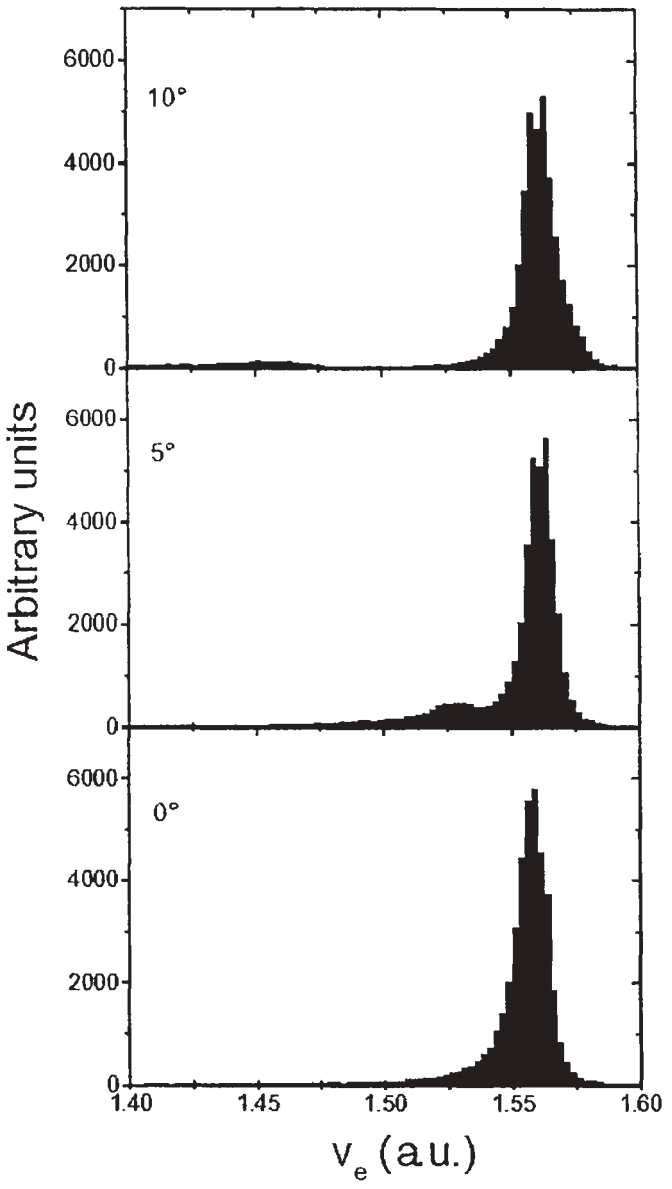

Fig. 5. Autoionization spectra as a function of the electron velocity for angles 0, 5 and 10°.

behavior could be due to the simple superposition of separate structures in agreement with recent quantum results [16].

4. Conclusions

In this work, we have performed a classical treatment of the autoionization process. Restricting ourselves to the post collisional interaction approach, we have assumed that the emitted electron only interacts with the projectile Coulomb center. A complete treatment of the problem would include the emitter Coulomb field.

The electron emission by autoionization of the target has been modelled by giving a profile in the initial velocity for the autoionizing electron as well as a probabilistic weight for the emission at different projectile distances. The final electron distributions in momentum space have been obtained using the classical trajectories and the statistical initial conditions. A comparison with the calculations resulting from the CDW quantum theory has been performed. When compared with the quantum mechanical method our classical model presents similar structures with nearly identical positions and forms. These are the autoionization and binary rings, and the focusing peak. Another non-classical structure has been observed which does not seem to be reproduced by the present model, probably due to a pure quantum origin. The autoionization peak profile has been obtained, exhibiting the correct asymmetry. The binary peak appears as a contribution of all the autoionizing electrons emitted at different times with an angle which allows them to cross the projectile trajectory. In this sense, the classical simulation procedure could be useful in order to distinguish purely quantum structures, as interference patterns, from the simply accumulation of classical ones.

It is our hope that the present study would contribute to a deeper understanding of the classical and semi-classical mechanisms inherent to the autoionization process with post-collisional-interactions.

Acknowledgments

The authors would like to thank C. R. Garibotti and F. D. Colavecchia for helpful discussions and for careful reading of the manuscript. This work has been partially supported by the PICT Grant No. 99/03/06249 of the APCYT and PGI Grant No. 24/F-027 of the UNS (Argentina).

References

1. Auger, P., J. Radium **6**, 205 (1925).
2. Barker, R. B. and Berry, H. W., Phys. Rev. **151**, 14 (1966).
3. Devdariani, A. Z., Ostrovskii, V. N. and Sebayakin, Yu. N., Sov. Phys. JETP **46**, 215 (1977).
4. van der Straten, P. and Morgenstern, R., J. Phys. B: At. Mol. Opt. Phys. **19**, 1361 (1986).
5. Barrachina, R. O. and Macek, J. H., J. Phys. B: At. Mol. Opt. Phys. **22**, 2151 (1989).
6. Swenson, J. K., Havener, C. C., Stolterfoht, N., Sommer, K. and Meyer, F. W., Phys. Rev. Lett. **63**, 35 (1989).
7. Miraglia, J. E. and Macek, J. H., Phys. Rev. A **42**, 3971 (1990).
8. Cordrey, I. L. and Macek, J. H., Phys. Rev. A **48**, 1264 (1993).
9. Otranto, S., Garibotti, C. R., Colavecchia, F. D. and Gasaneo, G., Phys. Rev. A **63**, 022713 (2001).
10. Swenson, J. K. *et al*., Phys. Rev. Lett. **66**, 417 (1991).
11. Samengo, I., Pregliasco, R. G. and Barrachina, R. O., J. Phys. B: At. Mol. Opt. Phys. **32**, 1971 (1999).
12. Kunikeev, Sh. D. and Senashenko, V. S., Sov. Phys. JETP **82**, 839 (1996).
13. Landau, L. D. and Lifshitz, E. M., ''Mecánica'' (Editorial Reverté, Barcelona, 1985).
14. Goldstein, H., ''Mecánica Clásica,'' (Editorial Reverté, Barcelona, 1990).
15. Cohen-Tannoudji, C., Diu, B. and Laloë, F., ''Quantum Mechanics,'' Vol. II (John Wiley & Sons, New York, 1977).
16. Caputti, K., Diploma Thesis, Centro Atomico Bariloche Library, Argentina (1998).
17. Della Picca, R., Barrachina, R. O. and Zitnik, M., XXIII Int. Conf. Physics of Electronic and Atomic Collisions, Stockholm, Sweden (2003).
18. Crooks, G. B. and Rudd, M. E., Phys. Rev. Lett. **25**, 1599 (1970).
19. Macek, J. H., Phys. Rev. A **1**, 235 (1970).
20. Samengo, I. and Barrachina, R. O., J. Phys. B: At. Mol. Opt. Phys. **29**, 4179 (1996).

